Strain rate dependent undrained shear strength response of soft Kandla soil

Shrweta Dutta [1*], *N. D. A Achintya* Pradhan [1], *Kusumika* Das [1], and *Ajanta* Sachan [1]

[1] Department of Civil Engineering, Indian Institute of Technology Gandhinagar, Gandhinagar, India

Abstract. The extensive coastal stretches of Gujarat are underlain by soft marine clays that are highly plastic, highly compressible, moisture-rich, and sensitive to remolding. These soft clays beneath onshore and offshore infrastructure are exposed to a range of diverse loading rates during their service life, which makes understanding the strain-rate-dependent shear strength behavior of these soils crucial for ensuring the stability and longevity of coastal infrastructure. The present study is focused on evaluating the monotonic undrained response of soft marine clay collected from Kandla Port, Gujarat, India. A series of unconfined compression and consolidated undrained triaxial tests were performed on slurry-consolidated specimens at different strain rates. The high strain rates of loading essentially simulated rapid loading scenarios, such as excavation, surcharge application, and the fast installation of piles and anchors. The experimental findings revealed distinct *isotach* behavior observed at all axial strain levels, characterized by unique rate-dependent stress-strain curves. An increase in the loading rate was found to reduce the undrained shear strength of the soil, quantified by determining the strength change rate (*R*). The study further analyzed pore pressure evolution, effective stress path, and maximum obliquity response. The influence of strain rate on the mechanical behavior of soft Kandla soil was also interpreted using strain energy dissipation mechanism.

1 Introduction

The rapid growth of infrastructure worldwide, both on land and offshore, has led to greater dependence on foundations built over marine deposits. These marine soils are generally soft, moisture-rich, and highly sensitive, characterized by high compressibility and low shear strength. In addition, they are particularly prone to time-dependent effects [1].

Numerous studies have shown that different geomaterials, such as sands, weathered rocks, and clays, respond differently to changes in strain rate [2–5]. Experimental investigations have explored the effect of strain rate on the mechanical behavior of clays, both natural and reconstituted. Some researchers have reported that increasing strain rate leads to higher mobilized shear strength and lower excess pore water pressure generation [1,6–13]. In contrast, other studies have observed an increase in pore pressure with increasing strain rate [14,15]. These contrasting findings highlight the complex nature of rate-dependent behavior in clays. Similarly, the effect of strain rate on the effective friction angle remains uncertain. While some studies have reported an increase in strength parameters with higher loading rates [16], others have documented a reduction in effective friction angle as strain rate increases [8]. Sudan and Sachan [8] investigated the combined influence of strain rate and confining pressure on the pore pressure evolution and effective stress path response of soft marine soil. Wu et al. [10,11] examined Macau marine clay under both K_0 and isotropic consolidation conditions and observed higher shear strength and reduced pore pressure at higher loading rates. Li et al. [15] further observed significant strain-hardening behavior, strength mobilization and pore pressure response in stiff clays subjected to step changes in strain rate.

Tatsuoka [17] proposed a conceptual framework to describe the strain rate dependency of geomaterials by classifying their behavior into three main types: *isotach*, *TESRA* (Temporary Effect of Strain rate and Acceleration), and a combined *isotach–TESRA* mode. The concept of *isotach* behavior was first introduced by Šuklje [18] and later refined through detailed experimental investigations by Leroueil [19] and Tatsuoka [17]. It provides a general approach to interpret how changes in strain rate influence the stress-strain response of soils. Although the concept was originally developed for one-dimensional consolidation, it was further extended to triaxial loading conditions and incorporated into advanced rate-dependent constitutive models [20,21]. Recent studies [1,13] have further indicated that soft clays exhibit *isotach*-type behavior during triaxial shearing, characterized by distinct stress-strain curves obtained at different strain rates.

The studies focused on the undrained shear strength response of natural soft clays under fully saturated conditions, particularly subjected to high strain rates, are

* Corresponding author: duttashrweta@iitgn.ac.in

comparatively limited in literature. The current study is based on investigating the strain-rate-dependent undrained behavior of the soft marine soil collected from Kandla Port, Gujarat, India. A series of consolidated undrained (CU) triaxial tests was conducted over a wide range of strain rates, varying from 0.005% per min to 9% per min. The effect of loading rate on stress-strain response, excess pore water pressure development, effective stress paths, and the maximum obliquity angle was examined. The variation in cumulative strain energy dissipation at different strain rates was also analyzed to provide a comprehensive understanding of the soil's rate-dependent response under saturated undrained conditions.

2 Material properties and specimen preparation

This study investigated the soil collected from Kandla Port, Gujarat, India. The grain-size distribution curve of the soil is shown in Fig. 1, indicating the presence of 36% clay and 64% silt. The soil had a liquid limit (w_L) of 70%, plastic limit (w_P) of 34%, and plasticity index (I_P) of 36%. The specific gravity (G_s) was obtained to be 2.80. Based on the Unified Soil Classification System, the soil was classified as a high-plasticity clay (CH). Scanning Electron Microscope (SEM) micrograph of the soil obtained at ×30,000 magnification is presented in Fig. 2. A free swell index (FSI) of 53% further signified the very high expansion potential of the soil [22].

In this study, the slurry-consolidation technique was used to reconstitute the soft Kandla soil specimen in the laboratory at its in-situ bulk density (1.64 g/cc) and in-situ water content (57%). The solid cylindrical specimens of the soil were prepared by mixing 900 g of oven-dried powdered soil with 1494 g of distilled water to form a clay slurry at 166% water content (approximately 2.4 times of w_L). The slurry was then consolidated under K_o-conditions at a vertical pressure of 120 kPa. Double drainage conditions were maintained throughout the consolidation process, and volume changes were continuously monitored. A consolidated soil cake measuring 97 mm in diameter and 110 mm in height was obtained after 96 hours of slurry consolidation. The average water content measured at the top, middle, bottom, and core sections of the soil cake was determined to be approximately 57%, confirming the uniformity and homogeneity of the prepared specimens at its in-situ conditions.

3 Experimental program

All the experiments were performed on cylindrical specimens of soft Kandla soil measuring 50 mm in diameter and 100 mm in height. These specimens were carefully extracted from the prepared slurry-consolidated soil cakes of 97 mm diameter and 110 mm height.

The effect of strain rate on the geotechnical behavior of soft Kandla soil was investigated by performing a series of triaxial compression tests. The Consolidated Undrained (CU) triaxial tests were performed over a wider range of axial strain rates, varying from 0.005% to 9% per min. Additionally, Unconfined Compression (UC) tests were also conducted at six axial strain rates of 0.5% per min, 1% per min, 1.25% per min, 1.5% per min, 2% per min, and 5% per min.

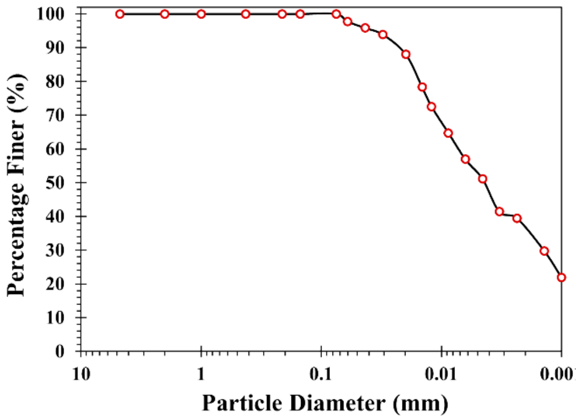

Fig. 1. Grain size distribution curve of soft Kandla soil.

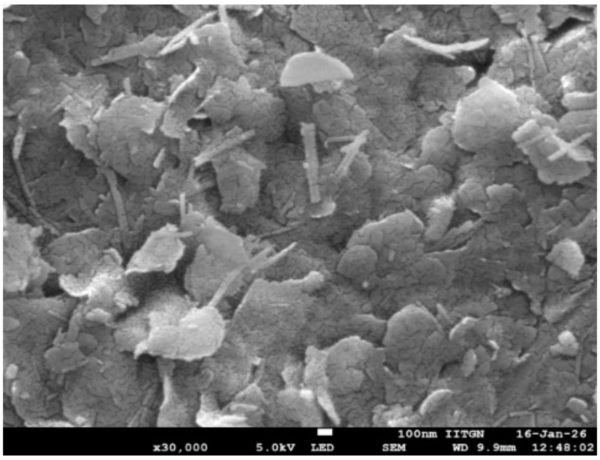

Fig. 2. SEM micrograph of soft Kandla soil.

In the CU triaxial tests, the soft soil specimens were mounted on the triaxial pedestal with porous stones and circular filter papers placed at both ends. In addition, six vertical filter paper strips were attached around the circumference of each specimen to facilitate radial drainage. This accelerated the saturation and consolidation processes in the CU triaxial tests on soft clay. Complete saturation was ensured when the Skempton's pore pressure parameter ($B = \Delta u/\Delta\sigma_c$) exceeded 0.95, which was achieved at a back pressure of 270 kPa in all the triaxial tests. The specimens were then isotropically consolidated to an effective confining pressure of 100 kPa and sheared under undrained conditions at four different axial strain rates of 0.005% per min, 0.05% per min, 5% per min, and 9% per min. The higher rates were selected to simulate rapid field loading conditions, such as deep excavations, sudden surcharge application, and high-speed pile or anchor installation [7,8,14,23].

4 Results and discussion

The undrained shear strength behavior of the soft Kandla soil was evaluated by conducting a series of Consolidated Undrained (CU) triaxial tests conducted at effective confining pressures of 50 kPa, 100 kPa, and 300 kPa. After isotropic consolidation, the specimens were sheared at an axial strain rate of 0.05% per min, ensuring uniform pore pressure distribution throughout the soil specimen. The resulting stress-strain behavior, pore pressure evolution, and effective stress path responses are presented in Fig. 3.

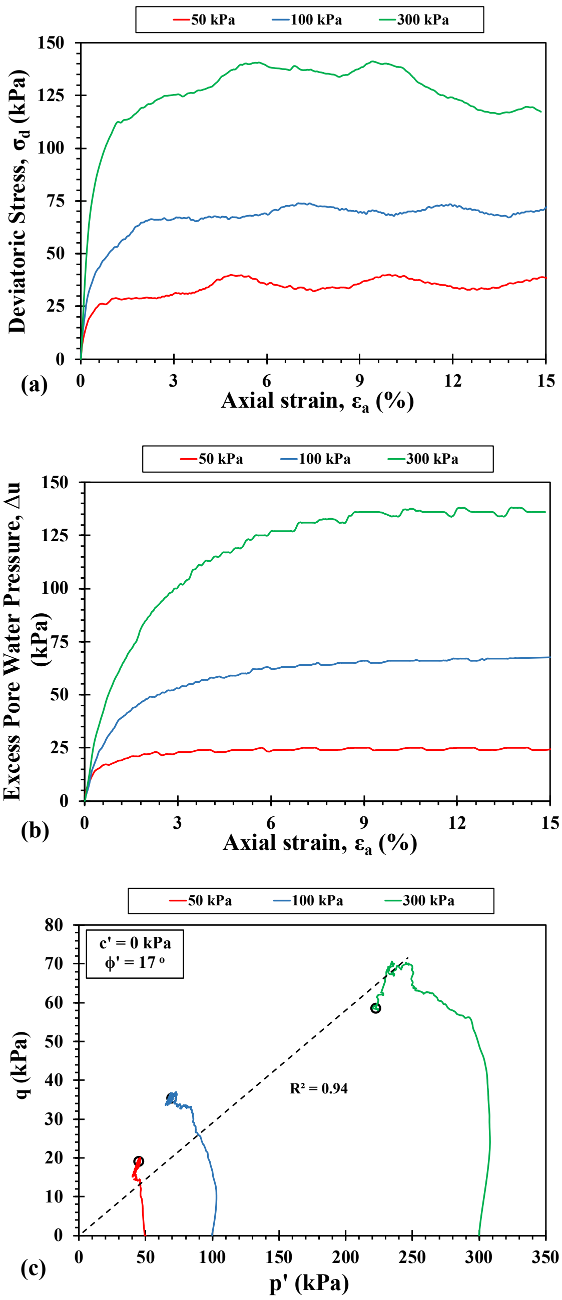

Fig. 3. Shear strength characteristics of soft Kandla soil: (a) stress-strain behavior, (b) excess pore pressure evolution, and (c) effective stress path response.

The stress-strain curves of the soft Kandla soil (Fig. 3(a)) displayed a distinct pattern of strength evolution, marked by an initial increase in strength, followed by softening and a gradual recovery. The ability of the soft soil to regain part of the strength lost during deformation is referred to as thixotropy, a time-dependent structural rearrangement commonly observed in cohesive soils. Ren et al. [24] reported that fully saturated, montmorillonite-rich soils exhibit thixotropic behavior due to the presence of salt content within the soil mass. In addition, this effect becomes significant in clays with water content close to their liquid limit [25–28]. In the current study, the marine soft Kandla soil contained dissolved salts and had a high water content of 57%, which is near its liquid limit of 70%. It also had montmorillonite clay mineral with high swelling potential (FSI = 53%). These combined factors contributed to the observed thixotropic behavior in soft Kandla soil. This study further employed a limiting axial strain failure criterion of 15% to determine the effective shear strength parameters, c' and φ', of the soft Kandla soil under undrained conditions [29,30]. The soil was observed to exhibit zero cohesion and an effective internal friction angle (φ′) of 17° (Fig. 3(c)).

The effect of strain rate on the unconfined compressive strength and initial stiffness of the soft Kandla soil was investigated. In addition, variations in stress-strain behavior, excess pore water pressure development, effective stress paths, and maximum obliquity response under different loading rates were evaluated through consolidated undrained triaxial tests. The cumulative strain energy dissipated at different strain rates was also determined for soft Kandla soil under undrained shearing conditions.

4.1 Rate-dependent unconfined compressive strength of soft Kandla soil

The variation of unconfined compressive strength (q_u) of the soft Kandla soil at axial strain rates ranging from 0.5% to 5% per minute is presented in Fig. 4. It was observed that the strain rate exerted no significant influence on the unconfined compressive strength of the soil. The axial stress-strain curves exhibited similar responses at all applied loading rates. Although minor variations in q_u were observed at different strain rates (Table 1), no consistent trend was identified. The initial stiffness of the soil was also found to remain largely unaffected by changes in the rate of loading.

Table 1. Unconfined compressive strength (q_u) and undrained cohesion (c_u) of soft Kandla soil under different strain rates.

Strain Rate (%/min)	q_u (kPa)	c_u (kPa)
0.5	31.4	15.7
1	31.3	15.7
1.25	31.6	15.8
1.5	30.1	15.1
2	35.0	17.5
5	32.8	16.4

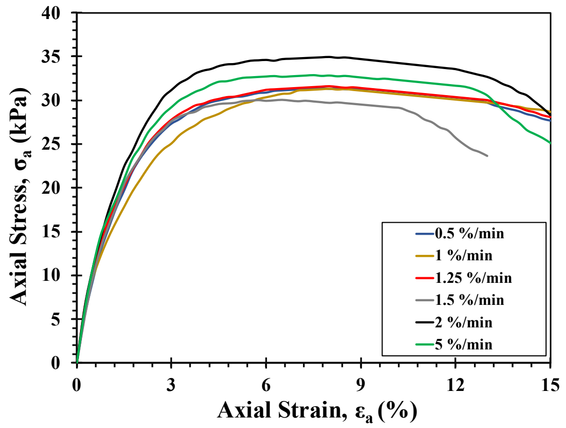

Fig. 4. Unconfined compressive strength of soft Kandla soil under varying strain rates.

4.2 Rate-dependent monotonic undrained shear strength response of soft Kandla soil

Fig. 5 illustrates the stress-strain behavior of the soft Kandla soil sheared at axial strain rates of 0.005%, 0.05%, 5%, and 9% per minute. It was observed that the soil exhibited an *isotach*-type of behavior over the entire axial strain range of 15%, with distinct stress-strain curves obtained at each loading rate. At a constant effective confining pressure of 100 kPa, an increase in strain rate resulted in a reduction in deviatoric stress. This response contradicted with several earlier studies, where higher loading rates were reported to enhance the strength of clays, independent of confining pressure [1,6,7,9–11,14,15]. In this study, the decrease in strength with increasing strain rates might be attributed to rapid shear stress mobilization, inducing localized deformation and disturbance of the soil fabric and ultimately reducing the shear resistance of the soil. Furthermore, the thixotropic effect was observed to persist even at the highest applied strain rate of 9% per minute. The onset of this effect was noted at approximately 1% axial strain and continued throughout the loading process up to 15% axial strain.

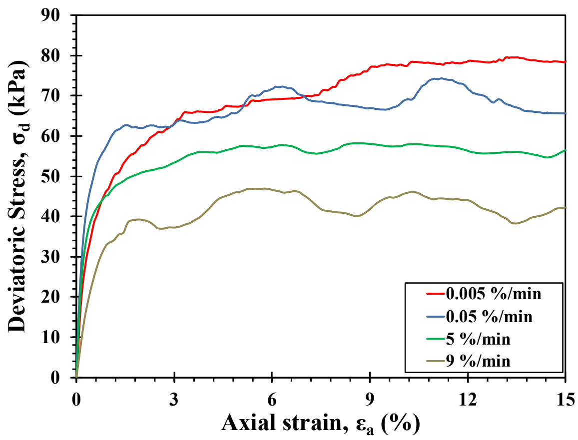

Fig. 5. Stress-strain behavior of soft Kandla soil under varying strain rates

The evolution of excess pore water pressure in the soft Kandla soil under different axial strain rates is depicted in Fig. 6. An increase in strain rate resulted in a decrease in excess pore pressure generation, demonstrating the significant influence of loading rate on the contractive behavior of the soil. A decrease in Δu of around 34% was noted at 15% axial strain for a rise in strain rate from 0.005 to 9% per min. Similar pore pressure responses have been reported for soft soils in previous studies [1,7,8,10,11]. The evolution of lower pore pressure at higher strain rates might be attributed to the development of non-uniform deformations within the soil mass. Such non-uniform and localized deformations would have contributed to the reduced contractive response of soil with increasing strain rates.

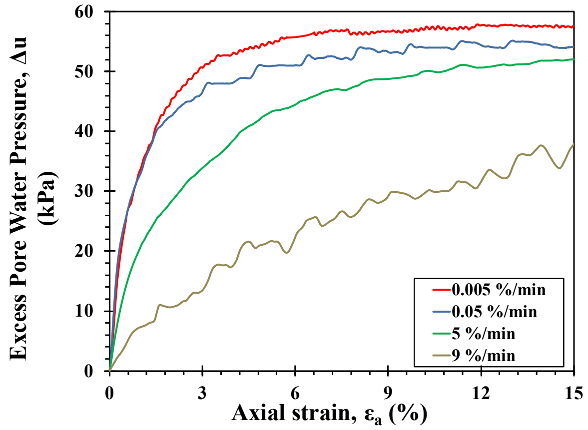

Fig. 6. Evolution of excess pore water pressure in soft Kandla soil under varying strain rates.

The evolution of the stress state during shearing is represented by the effective stress path (ESP) in the q - p' stress space, where the prevailing mean effective stress governs the resistance of the soil to applied loading [31]. The ESP responses of the soft Kandla soil subjected to different strain rates are shown in Fig. 7. In this study, the deviatoric stress (q) and mean effective stress (p') are defined as:

$$q = \frac{\sigma_1' - \sigma_3'}{2} \tag{1}$$

$$p' = \frac{\sigma_1' + \sigma_3'}{2} \tag{2}$$

where, σ'_1 and σ'_3 are the major and minor effective principal stresses during shearing, respectively. When the soft Kandla soil was sheared at a high strain rate (9% per minute), particle slippage occurred within localized regions, producing a relatively looser arrangement of clay and silt particles. With continued shearing, these weakened zones expanded and gradually propagated through the specimen. As multiple zones interconnected, localized failure might have initiated at an earlier stage in the high strain rate tests (9% per min) than in the low strain rate tests (0.005% per min). This caused the effective stress paths of the soil to progressive shift downward with increasing strain rate.

The influence of strain rate on the maximum obliquity angle (β_{max}) of the soft Kandla soil was also examined, as shown in Fig. 8. The angle of maximum obliquity (β_{max}) is defined as the maximum angle formed between the resultant stress vector and the normal stress vector, serving as an indicator of the extent of shear strength mobilized at a particular strain level. A consistent decrease in β_{max} was observed with increasing strain rate from 0.005% to 9% per min. This suggested that failure was mobilized at lower stress levels under higher loading rates. The rapid application of load at a high strain rate (9% per min) might have limited the time available for proper stress redistribution through interparticle contact points within the soil mass, leading to earlier failure compared to the specimen tested at a lower strain rate (0.005% per min).

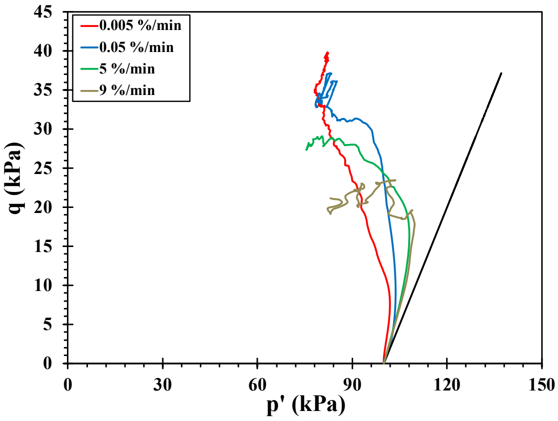

Fig. 7. Effective stress path response of soft Kandla soil under varying strain rates.

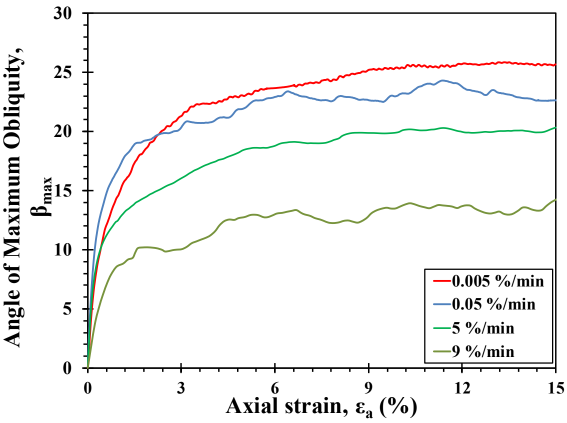

Fig. 8. Effect of strain rate on the maximum obliquity angle of soft Kandla soil.

Failure in this study was defined using a limiting axial strain failure criterion of 15%. The undrained shear strength (S_u) of the soft Kandla soil corresponding to 15% axial strain at different strain rates is listed in Table 2. The variation of S_u with strain rate is shown in Fig. 9(a) on a semi-logarithmic scale. It was found that the strength of the soft soil exhibited a negative trend with increasing strain rate. A decrease in shear strength of 46.11% was noted for a rise in strain rate from 0.005% per min to 9% per min.

The strain rate dependency of the undrained shear strength of the soft Kandla soil was further quantified by evaluating the strength change rate (R), using Equation (3) as:

$$R = \frac{S_u - S_{uo}}{S_{uo}} \times 100\% \quad (3)$$

where S_u is the undrained shear strength at a given strain rate (kPa) and S_{uo} is the strength measured at a reference strain rate (kPa). In this study, a reference strain rate of 0.05% per min was adopted, following Sachan and Penumadu [32]. The evaluated values of R for different strain rates are presented in Table 2 and plotted on a semi-log scale in Fig. 9(b). The results clearly indicated that an increase in loading rate led to a reduction in the undrained shear strength of the soft Kandla soil.

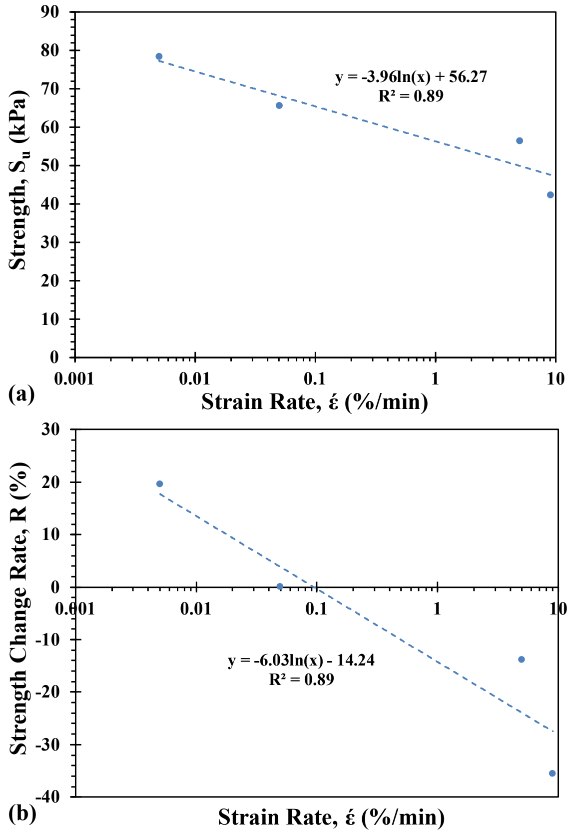

Fig. 9. Effect of strain rate on (a) undrained shear strength, and (b) strength change rate of soft Kandla soil.

Table 2. Strength characteristics of soft Kandla soil under varying strain rates.

Strain Rate (%/min)	S_u (kPa)	R (%)
0.005	78.5	20
0.05	65.6	0
5	56.5	-14
9	42.3	-36

The monotonic undrained shear behavior of the soft Kandla soil was also assessed using the strain energy dissipation framework. The total strain energy dissipated by the soil during shearing is a sum of the volumetric and shear strain energy components. It was computed following the formulation proposed by Tavenas et al. [33] as follows:

$$\delta W = \delta W_p + \delta W_q = (p' \times \delta\varepsilon_p) + (q \times \delta\varepsilon_q) \quad (4)$$

where, δW_p and δW_q represent the incremental volumetric and shear strain energies, respectively; $\delta\varepsilon_p$ is the incremental volumetric strain ($\delta\varepsilon_p = \delta\varepsilon_a + 2\delta\varepsilon_r$); and $\delta\varepsilon_q$ is the incremental shear strain ($\delta\varepsilon_q = 2(\delta\varepsilon_a - \delta\varepsilon_r)/3$). Under undrained triaxial conditions, the incremental axial strain is equal in magnitude and opposite in sign to twice the incremental radial strain, resulting in zero total volumetric strain.

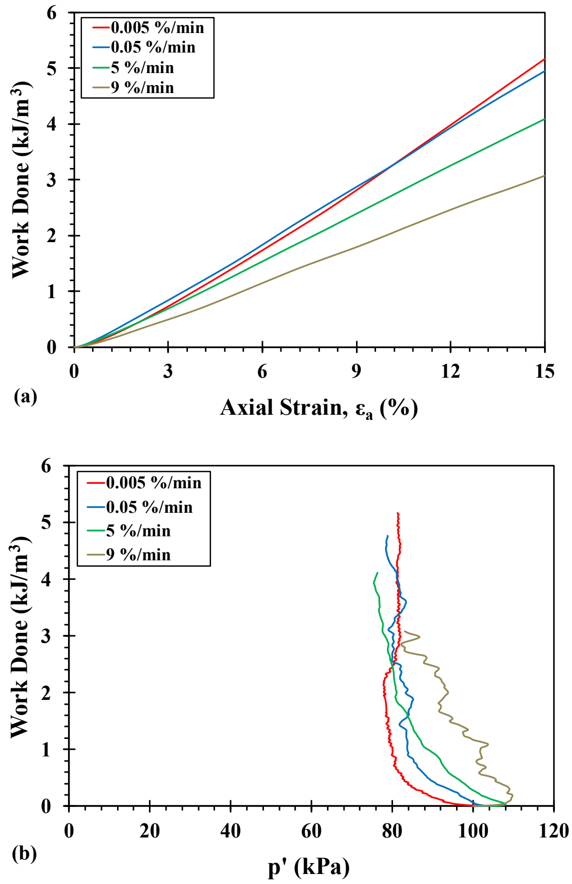

Fig. 10. Effect of strain rate on cumulative strain energy dissipation response of soft Kandla soil. (a) Total work done versus axial strain, and (b) Total work done versus mean effective stress.

Figs. 10(a) and 10(b) present the cumulative strain energy dissipated, in terms of total work done, plotted against axial strain (ε_a) and mean effective stress (p'), respectively, for different strain rates of undrained loading. A consistent reduction in total work done was observed as the strain rate increased from 0.005% per min to 9% per min, indicating lower strain energy dissipation at higher rates of loading. At 15% axial strain, the total dissipated energy was found to decrease by approximately 40%, reducing from 5 kJ/m³ at a strain rate of 0.005% per min to about 3 kJ/m³ at 9% per min. These observed responses suggested the occurrence of greater particle rearrangement in specimens during shearing at lower strain rates (0.005% and 0.05% per min). In contrast, higher rates of loading (5 and 9% per min) allowed limited internal adjustment of the soil structure, leading to reduced energy dissipation. The corresponding W - p' relationships displayed a steep upward trend, reflecting progressive increases in both volumetric stress and total strain energy dissipation in soft Kandla soil.

5 Conclusion

The current study explored the effect of strain rate on the undrained shear strength response of soft Kandla soil. The key findings derived from this study are summarized below:

1. The influence of strain rate on the unconfined compressive strength and initial stiffness of the soft Kandla soil was found to be negligible.
2. The soft soil exhibited *isotach* behavior, with distinct rate dependent stress-strain curves.
3. A continuous reduction in mobilized stress was observed as the strain rate increased from 0.005% to 9% per min. Thixotropic effect was further evident in the stress-strain responses of the soft soil at all strain rates, with the influence more pronounced at the highest loading rate of 9% per min.
4. Lower positive pore water pressure was generated within the soil with increasing strain rate, indicating a reduced contractive tendency of the soft Kandla soil under higher loading rates. This reduction in pore pressure caused a downward shift in the effective stress paths as the strain rate increased.
5. A decrease in the maximum obliquity angle was found with increasing strain rate, indicating early failure of soft soil under higher strain rates.
6. A significant reduction in the undrained shear strength of the soft Kandla soil was observed, decreasing from 78.5kPa at a strain rate of 0.005% per min to 42.3kPa at 9% per min. This was further reflected by the decreasing strength change rate (R), emphasizing the pronounced strain-rate-dependent undrained shear strength behavior of the soft soil.
7. Strain energy dissipation in the soft Kandla soil decreased with increasing strain rate. This suggested that under lower strain rates, the soft soil exhibited enhanced mechanical resilience to sustain higher stresses and dissipate more strain energy prior to failure.

The financial support and technical assistance provided by IIT Gandhinagar are gratefully acknowledged.

References

1. S.S. Torisu, J.M. Pereira, V. de Gennaro, P. Delage, A. Puech, Strain-rate effects in deep marine clays from the Gulf of Guinea. Geotechnique **62**(8), 695–706 (2012). https://doi.org/10.1680/geot.12.OG.015.
2. B.E. Martin, M.E. Kabir, W. Chen, Undrained high-pressure and high strain-rate response of dry sand under triaxial loading. Int. J. Impact Eng. **54**, 51–63 (2013). https://doi.org/10.1016/j.ijimpeng.2012.10.008.
3. M. Omidvar, M. Iskander, S. Bless, Stress-strain behavior of sand at high strain rates. Int. J. Impact Eng. **49**, 192–213 (2012). https://doi.org/10.1016/j.ijimpeng.2012.03.004.

4. A. Tsutsumi, H. Tanaka, Combined effects of strain rate and temperature on consolidation behavior of clayey soils. Soils Found. **52**(2), 207–215 (2012) https://doi.org/10.1016/j.sandf.2012.02.001.
5. K. Watanabe, O. Kusakabe, Reappraisal of loading rate effects on sand behavior in view of seismic design for pile foundation. Soils Found. **53**(2), 215–231 (2013). https://doi.org/10.1016/j.sandf.2013.02.003.
6. J. Graham, J.H.A. Crooks, A.L. Bell, Time effects on the stress-strain behaviour of natural soft clays. Geotechnique **33**(3), 327–340 (1983). https://doi.org/10.1680/geot.1983.33.3.327.
7. J.G. Zhu, J.H. Yin, Strain-rate-dependent stress-strain behavior of overconsolidated Hong Kong marine clay. Can. Geotech. J. **37**(6), 1272–1282 (2000). https://doi.org/10.1139/t00-054.
8. G.K. Sudan, A. Sachan, Effect of strain rate on pore pressure evolution and effective stress path of soft soil under different stress history conditions. Int. J. Geotech. Eng. **11**(1), 93–103 (2017). https://doi.org/10.1080/19386362.2016.1185844.
9. J. Han, C. Dano, P.-Y. Hicher, Z.-Y. Yin, Strain-rate dependency of shear strength for a highly overconsolidated clay. Geo-Congress 2014 Tech. Pap. **234**, 341–350 (2014). https://doi.org/10.1061/9780784413388.035.
10. S. Wu, T. Lok, Y. Xu, D. Wang, Rate-dependent behaviour of a saturated clay under different stress histories and k0 conditions. Acta Geotech. **15**(3), 679–694 (2020). https://doi.org/10.1007/s11440-019-00854-2.
11. S. Wu, T. Lok, Y. Xu, W. Wang, B. Wu, Rate-dependent behavior of a saturated reconstituted clay under different over-consolidation ratios and sample variance. Acta Geotech. **16**(11), 3505–3519 (2021). https://doi.org/10.1007/s11440-021-01293-8.
12. G. Lefebvre, P. Pfendler, Strain rate and preshear effects in cyclic resistance of soft clay. J. Geotech. Eng. **122**(1), 21–26 (1996). https://doi.org/10.1061/(asce)0733-9410(1996)122:1(21).
13. P.Q. Li, B.A. Baudet, Strain rate dependence of the critical state line of reconstituted clays. Geotech. Lett. **6**(2), 140–145 (2016). https://doi.org/10.1680/jgele.15.00140.
14. J.A. Díaz-Rodríguez, J.J. Martínez-Vasquez, J.C. Santamarina, Strain-rate effects in Mexico City soil. J. Geotech. Geoenviron. Eng. **135**(2), 300–305 (2009). https://doi.org/10.1061/(asce)1090-0241(2009)135:2(300).
15. Y. Liu, L. Luo, Y. Zhang, M. Lai, Y. Fu, Triaxial experimental study on strength characteristics of saturated soft soil under different shear strain rates. Lect. Notes Civ. Eng. **543** (2024). https://doi.org/10.1007/978-981-97-5814-2_14.
16. T.C. Sheahan, C.C. Ladd, J.T. Germaine, Rate-dependent undrained shear behavior of saturated clay. J. Geotech. Eng. **122**(2), 99–108 (1996). https://doi.org/10.1061/(asce)0733-9410(1996)122:2(99).
17. F. Tatsuoka, Inelastic deformation characteristics of geomaterial. Solid Mech. Its Appl. **146**, 1–42 (2007). https://doi.org/10.1007/978-1-4020-6146-2_1.
18. L. Šuklje, The analysis of the consolidation process by the isotaches method. Proc. 4th Int. Conf. Soil Mech. Found. Eng. 1, 200–206 (1957).
19. S. Leroueil, The isotache approach: Where are we 50 years after its development by Professor Šuklje? Proc. 13th Danube-Eur. Conf. Geotech. Eng. 1, 55–88 (2006).
20. Y. Watabe, S. Leroueil, Modeling and implementation of the isotache concept for long-term consolidation behavior. Int. J. Geomech. **15**(6) (2015). https://doi.org/10.1061/(asce)gm.1943-5622.0000270.
21. T.M. Bodas Freitas, D.M. Potts, L. Zdravkovic, A time dependent constitutive model for soils with isotach viscosity. Comput. Geotech. **38**(6), 809–820 (2011). https://doi.org/10.1016/j.compgeo.2011.05.008.
22. Bureau of Indian Standards, IS 2911 Part-3: Code of practice for design and construction of pile foundations, Part 3: Under-reamed piles. (1980).
23. T. Hu, D. Liu, J. Chang, Experimental study on strain rate effect of strength characteristics of unsaturated silty clay. Case Stud. Constr. Mater. **12**, e00332 (2020). https://doi.org/10.1016/j.cscm.2020.e00332.
24. Y. Ren, S. Yang, K.H. Andersen, Q. Yang, Y. Wang, Thixotropy of soft clay: A review. Eng. Geol. **287**, 106097 (2021). https://doi.org/10.1016/j.enggeo.2021.106097.
25. A.R. Shahriar, M.Z. Abedin, R. Jadid, Thixotropic aging and its effect on 1-D compression behavior of soft reconstituted clays. Appl. Clay Sci. **153**, 210–218 (2018). https://doi.org/10.1016/j.clay.2017.12.029.
26. S. Seng, H. Tanaka, Properties of very soft clays: A study of thixotropic hardening and behavior under low consolidation pressure. Soils Found. **52**(1), 1–13 (2012). https://doi.org/10.1016/j.sandf.2012.02.010.
27. R. Sinha, R.K. Ghanekar, Thixotropic properties of deepwater Indian marine clays from Eastern Offshore—evaluation and correlations. Lect. Notes Civ. Eng. **136**, 495–503 (2021). https://doi.org/10.1007/978-981-33-6370-0_46.
28. A.W. Skempton, R.D. Northey, The sensitivity of clays. Geotechnique **3**(1), 30–53 (1952). https://doi.org/10.1680/geot.1952.3.1.30.
29. ASTM International, ASTM D4767-20: Standard test method for consolidated undrained triaxial compression test for cohesive soils (2020).
30. T.L. Brandon, A.T. Rose, J.M. Duncan, Drained and undrained strength interpretation for low-plasticity silts. J. Geotech. Geoenviron. Eng. **132**(2), 250–257 (2006). https://doi.org/10.1061/(asce)1090-0241(2006)132:2(250).
31. S. Dutta, A. Khan, A. Sachan, Monotonic undrained and drained compression response of CL-ML soil. Eur. J. Environ. Civ. Eng. **30**(1), 1–26 (2025). https://doi.org/10.1080/19648189.2025.2584115.
32. A. Sachan, D. Penumadu, Effect of microfabric on shear behavior of kaolin clay. J. Geotech. Geoenviron. Eng. **133**(3), 306–318 (2007). https://doi.org/10.1061/(asce)1090-0241(2007)133:3(306).
33. F. Tavenas, P. La Rochelle, M. Roy, J.P. Des Rosiers, S. Leroueil, The use of strain energy as a yield and creep criterion for lightly overconsolidated clays. Geotechnique **29**(3), 285–303 (1979). https://doi.org/10.1680/geot.1979.29.3.285.